https://doi.org/10.5194/hess-2022-193
Preprint. Discussion started: 31 May 2022


Hydrology and Earth System Sciences
Discussions

# Modelling of water infiltration into water repellent soils

Claude Hammecker[1], Siwaporn Siltecho[2], Rafael Angulo Jaramillo[3], and Laurent Lassabatere[3]

[1]LISAH, Univ Montpellier, INRAE, IRD, Montpellier SupAgro, Montpellier, France.
[2]Land Development Department, Khon Kaen, Thailand
[3]Univ Lyon, Université Claude Bernard Lyon 1, CNRS, ENTPE, UMR5023 LEHNA, F-69518, Vaulx-en-Velin, France

**Correspondence:** C. Hammecker (claude.hammecker@ird.fr)

**Abstract.** Infiltration into water repellent soils has been widely observed, quantified and documented. The modelling of water infiltration into water repellent soils is more rarely taken into account explicitly. In this study, we modelled water infiltration into water repellent soils considering explicitly the contact angle, with the geometrical pore model proposed and validated previously. The applied microscopical approach showed good agreement with macroscopical models and with experimental data. We firstly investigated the case of contact angles lower than $90°$, for the cylindrical pore and pearl necklace (PN) models. The cumulative infiltrations were numerically generated versus contact angle and for different pore radii. Then, the modelled infiltration curves were fitted to the two-terms Philip equation and parameters $S$ and $A$, were evaluated versus contact angle. As predicted sorptivity $S$ decreased with increasing contact angle, and the constant infiltration rate $A$ increased with contact angle for both models. Then, the modelled data were fitted to numerical solution of Richards equation to derive the equivalent hydraulic parameters assuming van Genuchten model. The results showed that the contact angle decreased the saturated hydraulic conductivity and increased the parameter $\alpha$. Lastly, our model was used to investigate strong water repellency with contact angles higher than $90°$. Cumulative infiltration and related Philip parameters, $S$ and $A$, were evaluated versus water pressure head at surface $h_0$ and contact angles (between $90°$ and $96°$). Our model may be used to predict water infiltration into water repellent soils for both moderate and strong water repellency, including fingering features.

## 1 Introduction

Water repellent soils are widely distributed all over the world, in many different climates, and in different types of soils (DeBano, 2000; Dekker et al., 2005; Angulo-Jaramillo et al., 2016). Water repellent soils can be found under different types of covers, like turf grass, golf courses or in rubber tree plantations, or as a consequence of wildfire (Beatty and Smith, 2010; Nyman et al., 2010). Soil water repellency results generally from the presence of organic coating related to the presence of fungi, oily materials, resins in pine-woods, latex in rubber trees plantations, or any waxy material generally produced by plants. Ma'Shum et al. (1988) found that in water repellent soils, extensive polymethylene chains including both long-chain fatty acids and esters, were present. The waxy substances consist of long chain hydrocarbons, fatty acids and alkanes (paraffin-like compounds) (Mao et al., 2015). In water repellent soils of rubber-tree plantations, Le Besnerais (2011) found macromolecules with high molar mass of about $10^5 - 10^6 \mathrm{g.mol}^{-1}$ (7000 - 70000 C) which could correspond to poly(cis-1,4-isoprene), a major component of natural rubber with recognised hydrophobic properties.

https://doi.org/10.5194/hess-2022-193
Preprint. Discussion started: 31 May 2022


Hydrology and Earth System Sciences
Discussions
Open Access
EGU

Though water repellency does not impede completely infiltration into the soil, it is known to create water flow instability with development of fingering corresponding to preferential paths of infiltration (Ritsema et al., 1993; DeBano, 2000; Wang et al., 2000; Wallach and Jortzick, 2008). Despite being widespread, the problem of soil water repellency has mainly been described in these different situations: the problems of water infiltration have been measured experimentally, the non-zero contact angles have been assessed, but the actual infiltration has not been modelled. Bauters et al. (2000) showed that with a basic experimental setup, it is possible to characterise the imbibing front behavior by measuring the water entry pressure and the imbibing soil characteristic curve from the same heat treated, hence wettable soil. Bachmann et al. (2007) and Deurer and Bachmann (2007) proposed and tested successfully a model for water transfer in a soil of reduced wettability, where the changes in contact angle, are modelled by modification of parameter $\alpha$ in van Genuchten's retention equation (van Genuchten, 1980). More recently, precise geometrical studies of air-water interface progression into more or less complicated porous media, with different contact angles have been studied by Prodanović and Bryant (2006) and Jettestuen et al. (2013), though they didn't address directly infiltration kinetics. Infiltration kinetics into cylindrical tubes with different contact angle values, was computed numerically and compared to analytical solutions Chebbi (2007). More recently, a study based on gravity-flow infiltration into partly water repellent soils made of non uniform capillary tubes was investigated using Navier-Stockes equation showed the superiority of a sinusoidal pore model over cylindrical model Nissan et al. (2016).

In this paper, we propose a physical model based on previous studies about water infiltration into a geometrical porous network in which a single pore topology is taken into account (Hammecker et al., 1993; Hammecker and Jeannette, 1994; Hammecker et al., 2004). The aim of this paper is to give a theoretical insight on the water infiltration process into water repellent soils. We propose a mechanistic model based on a microscopical approach, where the pore geometry and the contact angle is explicitly taken into account, unlike other phenomenological studies relying on correction factors Abou Najm et al. (2021).

The aim of the proposed model is not to mimic the actual porous network geometry of soil with its complexity and variability, but to give a framework with a simplified geometry and topology defined by representative pore and pore neck radii to evaluate the infiltration properties. This model is basically an amelioration of the cylindrical model with the introduction of varying section determined similar to the model of sinusoidally constricted capillary channels of Beresnev et al. (2009).Basing on percolation threshold theory(Broadbent and Hammersley, 1957; Ghanbarian et al., 2013; Hunt, 2004), it was demonstrated that two representative radii giving access to the main part of the porous network, namely a threshold radius value for the pore access and a threshold radius for the pore size Hammecker et al. (2004) could describe the dynamics of water infiltration in sedimentary rocks and soils. The threshold value can also be assimilated to the water entry pressure, necessary to initiate infiltration (Baker, 1990; Geiger and Durnford, 2000; Glass et al., 1989). Therefore this model is not aimed at taking into account explicitly tortuosity and lateral interconnectivity, but at simulating the effect of water repellency on infiltration into an ensemble of capillary tubes. Besides, our infiltration model based on the percolation theory was compared with van Genuchten phenomenological approach with hydraulic parameters of unsaturated porous media and showed clear similarities. (Berkowitz and Balberg, 1992; Berkowitz and Ewing, 1998; Hunt, 2004; Hammecker et al., 2004; Mukunoki et al., 2016). Lastly, we investigated both moderate and strong water repellency, with respectively contact angles $\theta_w \leq 90\,°$ and $\theta_w > 90\,°$.

https://doi.org/10.5194/hess-2022-193
Preprint. Discussion started: 31 May 2022


Hydrology and Earth System Sciences
Discussions
Open Access
EGU

## 2 Theoretical background

Infiltration into porous network has been quantified according to many different models and approaches (Assouline, 2013; DiCarlo, 2013; Cai and Yu, 2011). The phenomenological method is the most commonly used for its convenience to use in a numerical resolution scheme. The 2-terms infiltration equation of Philip (1957) is one of the most popular model to quantify the 1D infiltration kinetics of water into the soil:

$$I = S \cdot \sqrt{t} + A \cdot t \tag{1}$$

which can be linearised:

$$\frac{I}{\sqrt{t}} = S + A \cdot \sqrt{t} \tag{2}$$

Where $I$ is the cumulative infiltration [L], $S$ the sorptivity [$\mathrm{L.T^{-1/2}}$] accounting for the capillary force and $A$ the constant infiltration rate parameter [$\mathrm{L.T^{-1}}$] accounting for gravity.

In the case of water repellent soils this formalism does not provide a suitable solution to quantify or model water infiltration. In many situations fitting Philip equation to infiltration curve into a water repellent soil would lead to a negative sorptivity value. Though mathematically suitable, according to the definition of Parlange (1975) negative sorptivity would physically be incorrect. More basic models related to the actual porous network, defined by its size and topology seem more suitable to describe this soil property.

### 2.1 The capillary model

In the most basic situation, considering the soil being constituted by a single capillary tube or a bundle of capillary tubes of similar size, it is possible to calculate the infiltration kinetics, according to a general equation derived from the Poiseuille's law (Sutera and Skalak, 1993):

$$Q = \frac{\pi \cdot r^4 \cdot \Delta P}{8 \cdot \eta \cdot z} = \frac{dV}{dt} = \frac{\pi \cdot r^2 \cdot dz}{dt} \tag{3}$$

$$dt = \frac{8 \cdot \eta \cdot z \cdot dz}{r^2 \cdot \Delta P} \tag{4}$$

where $Q$ is the water flow rate [$\mathrm{L^3T^{-1}}$] through the cylindrical tube of radius $r$, $dV$ is the volume variation, $\eta$ is the dynamic viscosity of water , $\Delta P$ is the total pressure difference between both ends of the capillary tube, and $z = Z_f$ [L] is the distance of the progressing meniscus from the free water level. In the case of water imbibition into the cylinder the driving pressure is a combination of the capillary pressure $P_c$ and the wetting front and gravity:

$$\Delta P = P_c + a \cdot \rho \cdot g \cdot z + \rho g h_0 \tag{5}$$

Where $\rho$ is the water density [$\mathrm{ML^{-3}}$], $g$ the gravitational constant [$\mathrm{LT^{-2}}$], z the height of the water column in the capillary [L], a is an integer depending on the water flow direction (+1: downwards, 0: horizontal, -1: upwards), $h_0$ is the pressure head [L] imposed at the capillary entrance (tension $h_0 < 0$ or ponding $h_0 > 0$ conditions).

https://doi.org/10.5194/hess-2022-193
Preprint. Discussion started: 31 May 2022


Hydrology and Earth System Sciences
Discussions
Open Access
EGU

According to Young-place equation Kutilek and Nielsen (1994), capillary pressure can be expressed as a function of the geometry of cylindrical tube and the interactions between the solid and the liquid phase, and equation 5 becomes:

$$\Delta P = \frac{2\sigma\cos\theta_w}{r} + a\cdot\rho\cdot g\cdot z + \rho g h_0 \tag{6}$$

With $\sigma$ being the surface tension [$MT^{-2}$], $\theta_w$ the contact angle of water with the capillary surface, $r$ the radius of the meniscus [L] which is equal to the capillary tube radius in this case.

Although Young-Laplace equation, describing the relation between capillary pressure and meniscus or cylinder radius Kutilek and Nielsen (1994), has been defined in hydrostatic equilibrium conditions, its has been used previously by Washburn (1921), Peiris and Tennakone (1980), Case (1990, 1994) to compute the motion of liquid into a capillary tube and validate these results against Navier-Stokes equations Dullien (1979). Combining equations 4 and 6 leads to:

$$dt = \frac{8\cdot\eta\cdot z}{(2\cdot r\cdot\sigma\cdot\cos\theta_w + r^2\cdot a\rho g z + \rho\cdot g\cdot h_0\cdot r^2)}\cdot dz \tag{7}$$

In the case of very water repellent conditions when $\theta_w > 90°$, and in order to avoid negative $dt$ values ($dt \geq 0$), and to avoid division by 0 a positive ponding pressure $h_0$ must be applied at soil surface at the beginning of the infiltration (z=0):

$$h_0 > \frac{-2\sigma\cos\theta_w}{r\rho g} \tag{8}$$

Equation 7 can then be integrated as follows:

$$\text{for } a = 0: \quad t = \left(\frac{4\eta}{2\cdot r\cdot\sigma\cdot cos(\theta_w) + \rho\cdot g\cdot h_0\cdot r^2}\right)\cdot z^2 \tag{9}$$

$$\text{for } a \neq 0: \quad t = \left[\frac{z}{ar^2\rho g} - \frac{2\sigma\cdot\cos\theta_w + \rho\cdot g\cdot h_0\cdot r}{a^2 r^3\rho^2 g^2}\cdot\ln\left(1 + \frac{ar\rho g z}{2\sigma\cdot\cos\theta_w + \rho\cdot g\cdot h_0\cdot r}\right)\right]\cdot 8\eta \tag{10}$$

For the case of vertical downwards infiltration (a=1), this equation is a general form of the well known Green-Ampt infiltration equation Green and Ampt (1911), commonly used in soil science when posing:

$$K_0 = \frac{\rho g r^2}{8\eta} \tag{11}$$

$$|\, h_f \,| = \frac{2\sigma\cos\theta_w + \rho g h_0\cdot r}{\rho g r} \tag{12}$$

Where $K_0$ [$L.T^{-1}$] is the saturated hydraulic conductivity and $|\, h_f \,|$ is the soil water head at the wetting front [L].

$$t = {K_0}^{-1}\left[z - |\, h_f \,|\ln\left(1 + \frac{z}{|\, h_f \,|}\right)\right] \tag{13}$$

In the usual treatment of these equations it is assumed that water is wetting perfectly the capillary or mineral surface so that $\theta_w$ is considered to be 0° and therefore the wettability is neglected. Although this approximation applies in most of the cases there are also numerous cases where it has to be taken into account (de Gennes, 1985). Thanks to this formalism it is possible to take into account the influence of the wettability, namely the variation of the contact angle, on the infiltration dynamics into a porous medium. Previous studies have taken into account wettability applied to Washburn law and compared the experimental response of increasing contact angle (e.g.,Czachor et al. (2010)).

https://doi.org/10.5194/hess-2022-193
Preprint. Discussion started: 31 May 2022


Hydrology and Earth System Sciences
Discussions

### 2.2 The "pearl necklace" model

Though the model composed of capillary bundles describes suitably the dynamics of infiltration into the soil, the cylinder radius has only a "hydraulic" signification without any physical relevance according to the actual pore size of the porous medium. In fact, when realistic pore radius values are introduced into equation 6, the calculated infiltration kinetics is higher than the experimental data by several orders of magnitude (Dullien, 1979; Hammecker et al., 1993).

A non cylindrical tube model composed of a stack of spheres similar to a pearl necklace (PN), defined by the radius of the sphere and the radius of the pore neck was consequently proposed and evaluated (Hammecker et al., 1993; Hammecker and Jeannette, 1994; Hammecker et al., 2004). In this conceptual model based on a geometrical representation of the porous network, the dimensions of necks and pore radii are realistic and determined experimentally by mercury intrusion, water retention curves and by direct measurements on thin sections. Therefore a radius $r(z)$ varying periodically between the pore access radius ($r_a$) and the pore radius ($R$) during infiltration was introduced in Equation 7 leading to:

$$dt = \frac{8\eta z \left(r(z)\right)^2}{r_a^4 \left(2\sigma \cos\theta_w / r(z) + \rho g \left(az + h_0\right)\right)} dz \tag{14}$$

where $r(z)$ is defined by the sphere shape (Figure 1) :

$$r(z) = \left(2Rz - z^2\right)^{1/2} \tag{15}$$

In the PN model the single element, is a truncated sphere of height $h_s$, where the meniscus progresses between $\epsilon_1$ and $\epsilon_2$ corresponding, respectively, to the upper and lower limit, where the access orifice cuts through the pore, with $\epsilon_1 = R + \sqrt{R^2 - r_a^2}$ and $\epsilon_2 = R - \sqrt{R^2 - r_a^2}$.

Similarly to equation 8, when $\cos\theta \leq 0$ and z=0, a minimal $h_0$ must be applied at the soil surface :

$$h_0 \geq \frac{2\sigma \cos\theta_w}{r(z=0)\rho g a} \tag{16}$$

The integration of equation 14 was resolved numerically with an iterative procedure, for small space intervals $dz$, as no analytical solution was available. The height of each spherical element $h_s$ is defined depending on both radii :

$$h_s = \epsilon_1 - \epsilon_2 = 2 \cdot \sqrt{R^2 - r_a^2} \tag{17}$$

For the numerical integration $dz$ was chosen to be $h_s/1000$, and simulation was performed over a total length $L$ of 0.2 m, within $L/h_s$ spherical elements.

### 2.3 Unsaturated soil characteristics

In the following, we describe an attempt to parametrise the hydraulic parameters in order to model water infiltration impacted by water repellency with Richard's equation. The cumulative infiltration curve $I(t)$ obtained with the cylindrical and pearl necklace models can be compared to water infiltration curves into soil or any other porous medium whether obtained experimentally or numerically computed with Hydrus 1D. The cumulative infiltrations obtained with our models were fitted to

https://doi.org/10.5194/hess-2022-193
Preprint. Discussion started: 31 May 2022


Hydrology and Earth System Sciences
Discussions

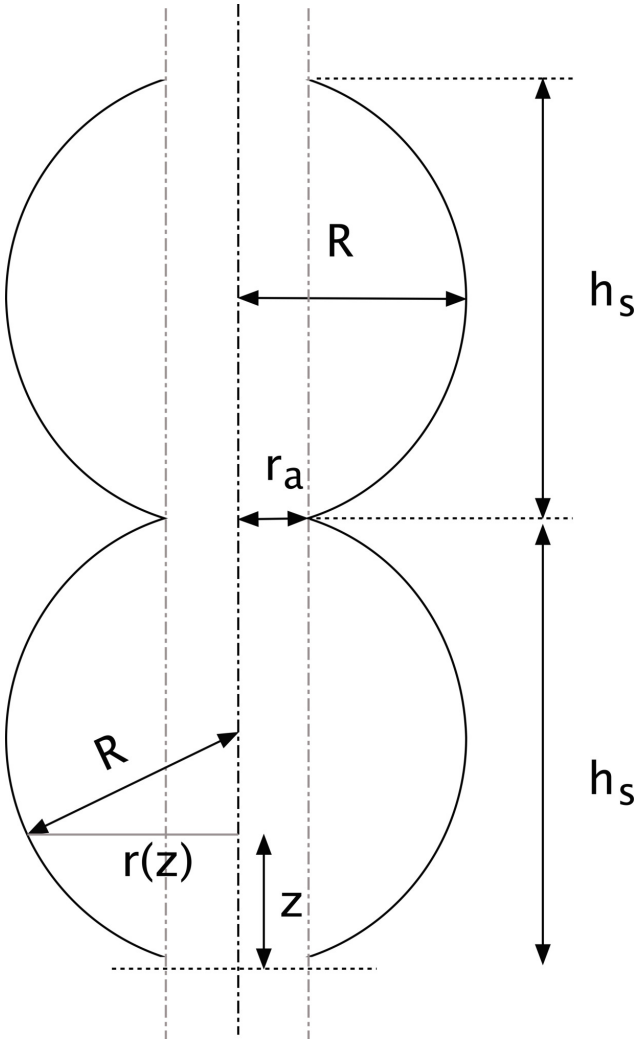


**Figure 1.** Representation of the pore space in the Pearl Necklace model

numerical solution of Richard's equation to optimise hydraulic parameters describing the water retention and the hydraulic conductivity functions. Therefore by modifying the contact angle in cylindrical and PN model it is possible to quantify the incidence of wettability on the main unsaturated soil parameters used in Richard's equation Richards (1931):

$$\frac{\partial\theta(h)}{\partial t} = \frac{\partial}{\partial z}\left[K(\theta)\left(1+\frac{\partial h}{\partial z}\right)\right] \tag{18}$$

Where the retention curve function $\theta(h)$ and the hydraulic conductivity function $K(\theta)$ are usually described with van Genuchten model van Genuchten (1980) and Mualem capillary model Mualem (1976), respectively:

$$S_e = \frac{\theta(h)-\theta_r}{\theta_s+\theta_r} = (1+(\alpha h)^n)^{-m} \tag{19}$$

https://doi.org/10.5194/hess-2022-193
Preprint. Discussion started: 31 May 2022


Hydrology and Earth System Sciences
Discussions

$$K(\theta) = K_s S_e^{1/2} \left(1 - \left(1 - S_e^{1/m}\right)^m\right)^2 \quad (20)$$

$S_e$ being the effective saturation, $\theta$ the volumetric water content, $\theta_r$ and $\theta_s$ the residual and saturated water content respectively, $K_s$ the saturated hydraulic conductivity, $\alpha$ a scale parameter, $m$ and $n$ shape parameters. Here these two parameters were considered as being related according to Mualem relationship ($m = 1 - 1/n$). The program Hydrus 1D Šimůnek et al. (2013) was used to evaluate these parameters for the computed infiltration curves, by inverse modeling. The domain was considered homogeneous with a depth of 1 m and the boundary conditions were set to constant pressure had (h=0) at the top, and free drainage at the bottom. The initial conditions were set to the values of activation of the tubes determined by $r_a$. The cumulative infiltration calculated by Hydrus 1D at the upper boundary, was fitted to the cumulative infiltration curve derived from the PN model, by adjusting the parameters $\alpha$ and $K_s$ following an internal Marquardt-Levenberg type procedure Šimůnek et al. (1998); Hopmans et al. (2002). The fits were considered only when $r^2$ for regression of predicted infiltration curve versus observed data was superior to 0.99. The number of parameters to be optimised has been set to two in order to reduce problems of equifinality and non uniqueness as the objective function is only a single infiltration curve. Considering that in the PN model the pore volume is described by a non uniform tube, $\theta_r$ and $\theta_s$ have been considered equal to 0 and 1 respectively and the shape parameter $n$ has been tested for various values usually found in soils (n = 2.1, 2.3, 2.5, 3) and an arbitrary high value, close to a Dirac distribution (n=8) to mimic the situation in the PN model; the main purpose being to assess the evolution of $K_s$ and $\alpha$ as the contact angle $\theta_w$ increased.

## 3 Results

### 3.1 Study of moderate water repellency - $\theta_w \leq 90°$

#### 3.1.1 Cylindrical model for $\theta_w \leq 90°$

The cumulative infiltrations decrease with increasing value of the contact angle $\theta_w$ (Figure 2), regardless of the geometry of pores (either cylindrical or PN). Such a results was expected considering that capillary pressure declines when wettability is reduced. The linearised graphs following equation 2 (i.e., $I/\sqrt{t} = f(\sqrt{t})$) show clearly the decreasing intercept value on the Y-axis, illustrating the decrease of sorptivity $S$ with increasing contact angle $\theta_w$.

On the other hand, the slope of the infiltration curves in the linearised graph (figure 2 b.), illustrating the constant infiltration rate parameter $A$, increased concomitantly with the contact angle between 0 and 90 °. When the relative sorptivity $S/S_0$, where $S_0$ stands for the usual sorptivity related to $\theta = 0°$, was considered, a unique relationship with the cosine of the contact angle $\cos(\theta)$ could be defined, regardless of the radius of the cylinder (figure 3). An equivalent relationship could also be defined for the relative constant rate $A/A_0$ as a function of $\cos(\theta)$, though for high angle values this relationship was not strictly unique and was also dependent on the capillary radius. The general shape of this relationship was a power function $S/S_0 = a_1 + a_2 \cdot (\cos(\theta))^{a_3}$ and, unexpectedly, it was significantly different from a direct contact angle correction of sorptivity

https://doi.org/10.5194/hess-2022-193
Preprint. Discussion started: 31 May 2022


Hydrology and Earth System Sciences
Discussions

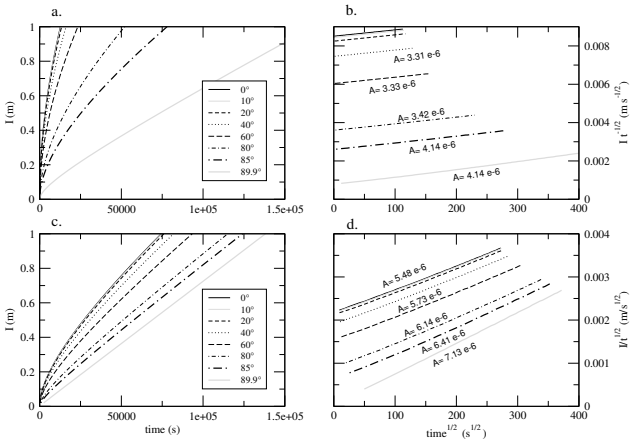


**Figure 2.** Infiltration curves computed for both cylindrical model (a. and b) and PN model (c and d), for different contact angles. The slope A of equation 2 is mentioned for different contact angle values (b. and d.), for a pore radius of $2 \cdot 10^{-6}$m for the cylindrical model versus $r_a = 8 \cdot 10^{-6}$m and R = $50 \cdot 10^{-6}$m for the PN model.

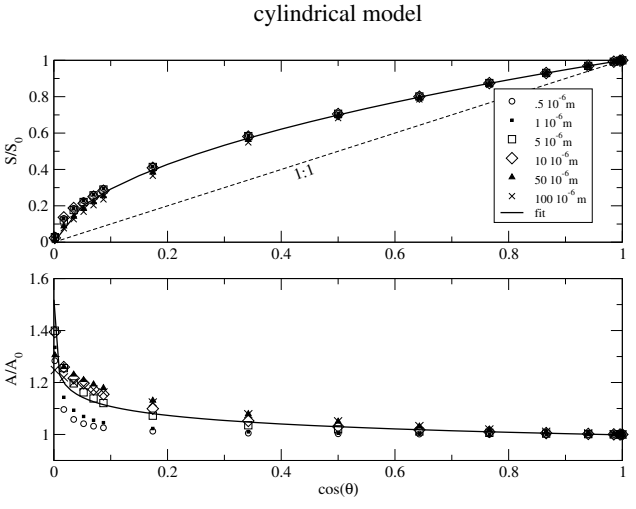


**Figure 3.** Evolution of relative sorptivity ($S/S_0$) and relative constant rate ($A/A_0$) versus the cosine of contact angle for the cylindrical model. The 1:1 line represents the direct angular correction $S_0 \times \cos(\theta)$ the symbols represent several cylinder radius.

$S_0 \cdot \cos(\theta)$ as shown in figure 3, with a maximum difference for a contact angle of 75°($\cos(\theta) = 0.25$). This result suggests that the correction of $S_0$ is close to a square root of the the cosine of the contact angle as confirmed by the values of the parameters of the empirical relationship $S/S_0 = f(\cos(\theta_w))$ listed in table1.

https://doi.org/10.5194/hess-2022-193
Preprint. Discussion started: 31 May 2022


Hydrology and Earth System Sciences
Discussions

**Table 1.** Empirical parameters for the relationship: $Y = a_1 + a_2 \cdot (\cos(\theta))^{a_3}$, $Y$ being $S/S_0$ and $A/A_0$

| cylindrical | $a_1$ | $a_2$ | $a_3$ | $r^2$ |
|---|---|---|---|---|
| $S/S_0$ | -3.86·10$^{-3}$ | 1.00 | 0.49 | 0.999 |
| $A/A_0$ | 1.33 | -0.34 | 0.198 | 0.89 |
| Pearl necklace | $a_1$ | $a_2$ | $a_3$ | $r^2$ |
| $S/S_0$ | -4.49·10$^{-2}$ | 1.047 | 0.519 | 0.999 |
| $A/A_0$ | 1.414 | -0.417 | 0.207 | 0.995 |

This corrective relationship of $S_0$ versus $\cos\theta$ could also be established by the integration of equation 7 when infiltration is horizontal ($a = 0$), without ponding pressure ($h_0 = 0$):

$$z = \sqrt{\frac{t \cdot \sigma \cdot \cos\theta \cdot r}{2 \cdot \eta}} = S \cdot \sqrt{t} \tag{21}$$

$$S/S_0 = \sqrt{\cos\theta} \tag{22}$$

This agreement between our numerical computations and the corrective relation and the mathematical derivations, i.e., Eq. 22 , make us confident on the quality of the numerical generation of the modelled cumulative infiltrations.

The relationship for the constant rate infiltration $A/A_0$ shows an increase with increasing contact angle (decreasing cosine), indicating an easier gravitational water flow with water repellency. When getting closer to 90°, the gravitational water flow ratio tends towards 1.4:

$$\lim_{\cos\theta \to 0} A/A_0 = 1.4 \simeq \sqrt{2}$$

This mathematical relationship is in line with the hypothesis of the decrease of the adhesive forces and therefore frictions onto the walls of the tubes when wettability decreases. As reported by Huang et al. (2008) or Neto et al. (2005) in a general review, slipping of water molecules along the walls of pores has been described for decreasing wettability by several authors. An alternative interpretation could be due to the use of truncated infiltration equation of Philip that is a simplified representation. In fact, when approximating a solution of Richards equation with the Philip equation, the parameter $A$ will not be a constant but increase over time for some time period. But even in that condition, the effect of increasing contact angle leads to an increase of infiltration time, with a consequently increase of $A$. The co-evolution of the two parameters $S/S_0$ and $A/A_0$ shows that the water repellency, as it is modelled in our approach, may at the same time decrease the capillarity-driven water infiltration and increase the gravity-driven water infiltration. This result is one of the novelty of this study.

#### 3.1.2 "Pearl necklace" model for $\theta_w \leq 90°$

The modelling has been performed with couples of pore-access and pore radii ($r_a, R$), commonly found in soils Hammecker et al. (2004), and with different proportionality ratio ($R/r_a$ = 5, 10, 20, 50, 100). The general trend for the PN model is

https://doi.org/10.5194/hess-2022-193
Preprint. Discussion started: 31 May 2022


Hydrology and Earth System Sciences
Discussions

equivalent to the cylindrical model showing a decrease of relative sorptivity $S/S_0$ with decreasing cosine of contact angle, as shown in Figure 4. The equation of the average relationship is only very slightly different from the cylindrical model (Table 1), close to a square root model.

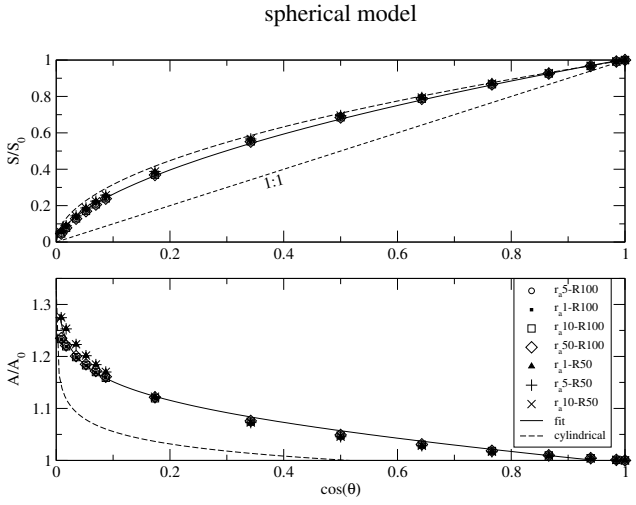


**Figure 4.** Evolution of relative sorptivity ($S/S_0$) and relative constant rate ($A/A_0$) versus the cosine of contact angle for the spherical (PN) model. The 1:1 line represents the direct angular correction $S_0 \times \cos(\theta)$. The dotted line represent the average relationship for the cylindrical model. The symbols represent several combinations of access and pore radii $(r_a, R)$.

Results for the relative constant infiltration rate ($A/A_0$) also followed a similar trend as described for the cylindrical model, but the results of modelling was less dependent on the size of pores than for the cylindrical model (Figure 4 versus Figure 3). Moreover it diverges notably from the relationship determined for the cylindrical model, showing a higher relative constant infiltration rate even for low contact angle as shown by the parameters determined in Table 1, but also reaching a value of $\sqrt{2}$ when $\cos\theta_w \rightarrow 0$. The PN model with varying pore radius has greater influence on the infiltration parameters and especially on the constant rate parameter $A$, mainly driven by gravity.

### 3.1.3 Influence of infiltration duration on evaluation of infiltration parameters

Evaluation of infiltration kinetics with the two first parameters ($S$ and $A$) of the Philip equation is an approximation of a power series ($I = \sum_{n=1,2,3,..} C_n \cdot t^{n/2}$) which in most cases is satisfactory. However one of the drawbacks of this approximation is that the evaluation of parameters $S$ and $A$ may depend on the infiltration duration. As increasing water repellency increases infiltration duration, evaluation of these parameters may be affected by this bias. To evaluate the effect of this numerical bias over water repellency, we computed the infiltration for cylindrical and PN models with increasing contact angle, and we determined parameters S and A for different infiltration times. Results displayed in figure 5 show that parameter $A$ is dependent on infiltration time for both models, whereas sorptivity ($S$) is hardly affected. The influence of infiltration duration appears to be slightly more important for the cylindrical model than for the PN model. Nevertheless, in both cases the effect of water

https://doi.org/10.5194/hess-2022-193
Preprint. Discussion started: 31 May 2022


Hydrology and Earth System Sciences
Discussions

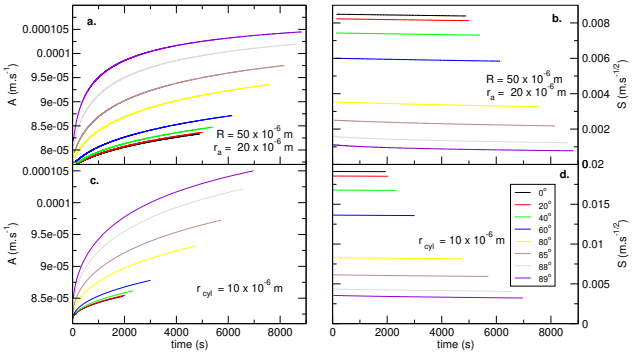


**Figure 5.** Evolution of infiltration parameters with time: **a.** constant infiltration rate for PN model,**b.** sorptivity for PN model, **c.** constant infiltration rate for cylindrical model, **d.** sorptivity for cylindrical rate.

repellency, especially when the contact angle is superior to 60°, is noticeably more important than the effect of infiltration time. Though the evaluation of constant infiltration rate $A$ is subjected to a numerical bias linked to the duration of infiltration, A undoubtedly increases with the increase of water repellency.

### 3.1.4 Evolution of VG parameters with contact angle for $\theta_w \leq 90°$

The determination by inverse modelling with Hydrus-1D of the two major van Genuchten parameters ($\alpha$ and $K_s$) showed different evolution with increasing contact angle. Continuous relationships could be drawn between the VG parameters $\alpha/\alpha_0$ and $K_s/K_{s0}$ and wettability (cosine of contact angle) as shown in figure 6.This figure demonstrates that $\alpha/\alpha_0$ increased with the contact angle, with an inverse function relating $\alpha/\alpha_0$ to $\cos(\theta_w)$. In their theoretical approach Bachmann et al. (2007) also found an inverse relationship between parameter $\alpha$ and the cosine of contact angle. These results illustrate the reduction of the apparent hydraulically active pore size with increasing contact angle. Regarding hydraulic conductivity, this figure demonstrated the decrease in $K_s$ when the contact angle is increased, i.e., when $\cos(\theta_w)$ is decreased. However, this decrease seems tiny and supports the fact that $K_s$ should not be dependent of the contact angle, as being determined in saturated conditions without interfaces. Such a result contradicts a little bit with what was mentioned previously, i.e., the increase of gravity-driven infiltration with water repellency. Note that for the case $n = 8$, the trends are more marked with significant increase in $\alpha_0/\alpha$ and decrease in $K_s/K_{s0}$. These results show that for the case of narrow pore size distribution with one single pore size, similar trends are confirmed but the magnitudes are increased.

For the case of $n \leq 3.5$, the following power relation was established to describe the evolution of these two parameters with water repellency:

$$\alpha/\alpha_0 = 1.0039 \cdot \cos(\theta_w)^{-0.9525} \tag{23}$$

https://doi.org/10.5194/hess-2022-193
Preprint. Discussion started: 31 May 2022


Hydrology and Earth System Sciences
Discussions

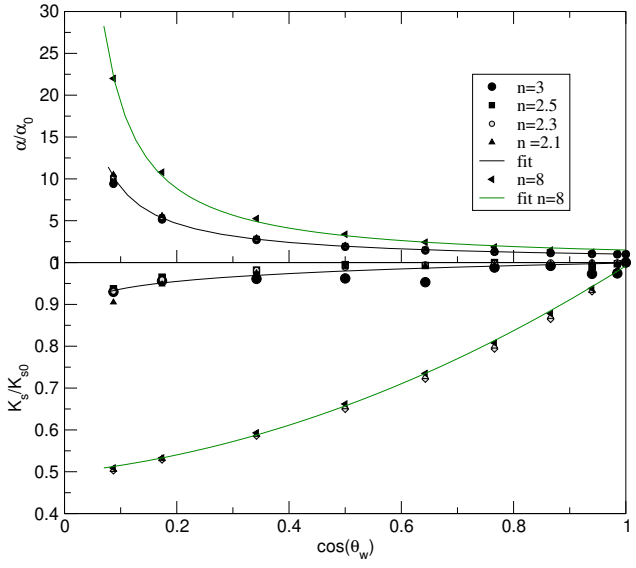


**Figure 6.** Evolution of adjusted relative van Genuchten's parameters $\alpha/\alpha_0$ and $K_S/K_{S0}$ with wettability (cosine of contact angle) for different values of parameter $n$

where $\alpha/\alpha_0$ is the relative empirical scale parameter of van Genuchten, where $\alpha_0$ is the reference value for $\theta_w = 0°$. For the relative saturated hydraulic conductivity $K_s/K_{s0}$ the following relation was obtained:

$$K_s/K_{s0} = 0.9989 \cdot \cos(\theta_w)^{0.028} \tag{24}$$

where $K_{s0}$ refers to the value of $K_s$ for $\theta_w = 0°$. For the case of high values of $n$ like $n = 8$, the relationships adapt to more marked trends:

$$\alpha/\alpha_0 = 1.49 \cdot \cos(\theta_w)^{-1.1} \tag{25}$$

$$K/K_0 = 0.35 \cdot \cos(\theta_w)^2 + 0.146 \cdot \cos(\theta_w) + 0.497 \tag{26}$$

This set of empirical equations represent a mean to simulate water repellency implicitly with a common water flow model like Hydrus. These equations define the effective hydraulic parameters to consider for the modeling of water infiltration into soil with the Darcean approach and the resolution of Richards' equation.

The trends obtained with the numerical inverse modeling may be interpreted in light of the previous results obtained with the fit to the two-terms infiltration equations (see Eq. 1 and Eq. 2 ) in the previous sections. The increase in $\alpha$ and the decrease in $K_s$ with water repellency are in line with the decrease in sorptivity obtained with the previous results. Conversely, the previous results indicated an increase in hydraulic conductivity, in relation with the increase of the term $A$ with water repellency whereas the numerical inverse modelling predicts the opposite trends. We have no specific explanation of hypothesis for this discrepancy.

https://doi.org/10.5194/hess-2022-193
Preprint. Discussion started: 31 May 2022


Hydrology and Earth System Sciences
Discussions

We may elaborate on the fact that the inverse modeling predicts at the same time the increase in the pore size (increase in $\alpha$) and the decrease in the hydraulic conductivity with water repellency when the analytical modeling (fit to the two-term analytical models) predicts an increase in the hydraulic conductivity, which is more consistent with larger pore sizes. It should be borne in mind that the water repellency does not change the porous medium structure but changes only the class of pores that are activated and that conduct flow (referred to as the hydro-dynamically active pores).

### 3.2 Cylindrical and PN models for strong water repellency - $\theta_w > 90°$

So far, we considered intermediate values for the contact angle, $\theta_w \leq 90°$. In this section, we address the case of very strong water repellency, i.e., when $\theta_w > 90°$. In the last case, spontaneous infiltration is theoretically impossible. Therefore a ponding water pressure head $h_0$ needs to be applied at the soil surface in order to counterbalance the repulsive pressure due to the hydrophobic effect. The results have been presented considering a relative ponding water pressure head, i.e., above the minimum pressure necessary to counterbalance the repulsive pressure of contact angle:

$$h_0^* = h_0 + \frac{2\sigma\cos\theta_w}{r^*\rho g} \tag{27}$$

with $h_0 \geq |2\sigma\cos\theta_w / r^*\rho g|$ and $h_0^* \geq 0$.

For the cylindrical model $r^*$ is the pore radius $r$ and for the PN model it corresponds to the pore access radius $r_a$. Any increase of contact angle is counterbalanced by the ponding pressure head ($h_0^*$). For each contact angle $\theta_w$ value, infiltration follows the same pattern with regular concave shapes that were fitted to equation 2 to get the estimates of sorptivity $S$ and coefficient A. The evolution of the relative sorptivity ($S/S_0$) and the infiltration rate ($A/A_0$) with increasing relative ponding pressure head ($h_0^*$) is shown in Figure 7. We chose to test contact angles $\theta_w$ only up to $95°$, because the compensating ponding water pressure head $h_0$ would exceed plausible height ($> 0.5$m) for these pore radii ($5 \cdot 10^{-6} < r < 20 \cdot 10^{-6}$m). Above this threshold, unrealistic values of water pressure head $h_0$ would be required to active the water infiltration.

These trends show a decrease in $A/A_0$ with $h_0^*$, and at the same time an increase in $S/S_0$ depending on the pore radius $R$. Regardless of the value of the contact angle greater than 90°, for each cylindrical radius the results align along the same curve. Different relationships can be defined for each capillary radius value $R$ , in particular for $S/S_0$ whereas $A/A_0$ align on the same curve regardless the value of $R$ (see Figure 7a). Empirical relationships to describe the evolution of $A/A_0$ and $S/S_0$ with the relative ponding pressure head $h_0^*$, with the following general form:

$$Y = a_1 + a_2 \cdot (h_0^*)^{a_3} \tag{28}$$

where Y represents $A/A_0$ and $S/S_0$. The parameters $a_1$, $a_2$ and $a_3$ were determined for several radii and displayed in table 2. The influence of $h_0^*$ over $A/A_0$ and $S/S_0$ is higher for the small values of $h_0^*$. Our result show that the effect of the two variables water pressure head $h_0$ and $2\sigma\cos\theta_w / r^*\rho g$ that corresponds to the effect of water repellency lump into one single key variable, $h_0^*$. $h_0^*$ is the main variable to compute to determine the resulting cumulative infiltration.

In the case of PN model, for contact angles close to 90°the infiltration curve displayed an inverted shape (figure 8), which corresponds to what is usually observed in field experiments on water repellent soils (Beatty and Smith, 2010; Lassabatere et al., 2012; Lassabatere et al., 2010).

https://doi.org/10.5194/hess-2022-193
Preprint. Discussion started: 31 May 2022


Hydrology and Earth System Sciences
Discussions
Open Access
EGU

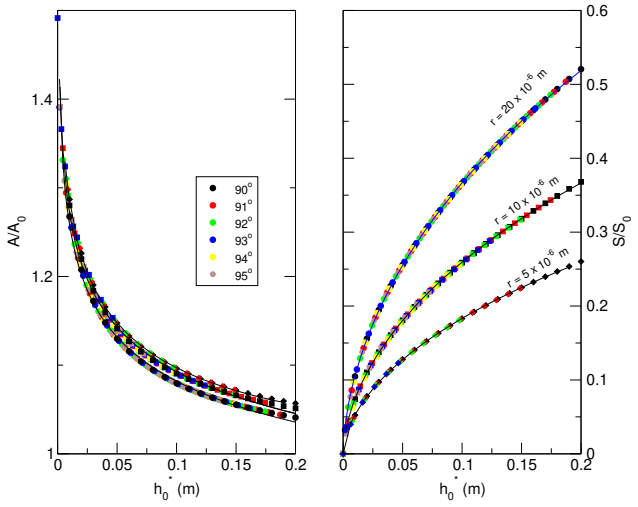


**Figure 7.** Evolution of the relative sorptivity $S/S_0$ and relative constant rate $A/A_0$ versus relative ponding pressure $h_0^*$ for the cylindrical model with several radii corresponding to the different curves, lumped together for $A/A_0$ and clearly spread apart for $S/S_0$

.

**Table 2.** Empirical parameters for the relationships with cylindrical model $Y = a_1 + a_2 \cdot X^{a_3}$ (Figure 7), and PN model $Y = a_1 + (a_2 - a_1)/(1 + (a_3/x)^{a_4})$ (Figure 10), $Y$ being the relative sorptivity $S/S_0$ and the relative constant rate $A/A_0$, and $X$ representing the relative ponding pressure $h_0^*$. For the PN model the pore radius was R = 50 $\cdot 10^{-6}$ m and $r_a = 20 \cdot 10^{-6}$m.

| cylindrical | r (m) | $a_1$ | $a_2$ | $a_3$ | |
|---|---|---|---|---|---|
| $S/S_0$ | $5 \cdot 10^{-6}$ | -0.234 | 0.768 | 0.570 | |
| $A/A_0$ | | 0.12 | 0.916 | -0.073 | |
| $S/S_0$ | $10 \cdot 10^{-6}$ | -0.331 | 1.086 | 0.570 | |
| $A/A_0$ | | 0.029 | 0.933 | -0.067 | |
| $S/S_0$ | $20 \cdot 10^{-6}$ | -0.846 | 1.806 | 0.602 | |
| $A/A_0$ | | 0.026 | 0.926 | -0.067 | |
| Pearl necklace | $\theta_w$ | $a_1$ | $a_2$ | $a_3$ | $a_4$ |
| $S/S_0$ | 90° | 0.0372 | 3.297 | 1.134 | 0.696 |
| $A/A_0$ | | 1.419 | 0.922 | 0.018 | 0.675 |
| $S/S_0$ | 91° | 0.112 | 3.415 | 1.406 | 0.694 |
| $A/A_0$ | | 1.284 | 0.919 | 0.0341 | 0.701 |
| $S/S_0$ | 95° | 0.2932 | 3.193 | 1.228 | 0.801 |
| $A/A_0$ | | 1.139 | 0.908 | 0.099 | 0.753 |

When $h_0$ reached higher values the shape of infiltration curve became concave as generally expected, and the usual Philip's parameters ($S$ and $A$) could be determined, still by fitting to equation 2. When represented versus the ponding pressure head

https://doi.org/10.5194/hess-2022-193
Preprint. Discussion started: 31 May 2022


Hydrology and Earth System Sciences
Discussions
Open Access
EGU

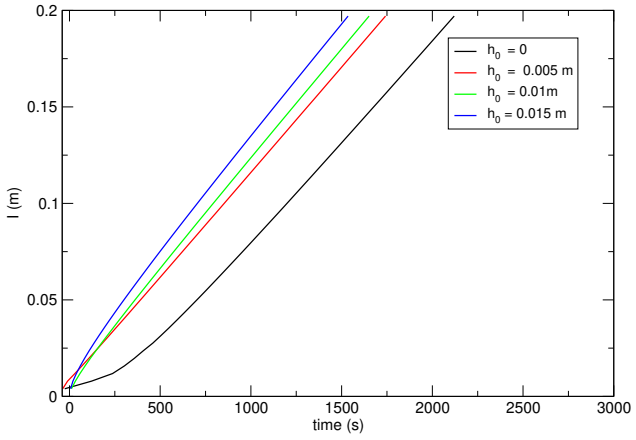


**Figure 8.** Infiltration curve for PN model ($r_a = 20 \cdot 10^{-6} m$, $R = 50 \cdot 10^{-6} m$, $\theta_w$ = 92 °) for several ponding pressure values $h_0$

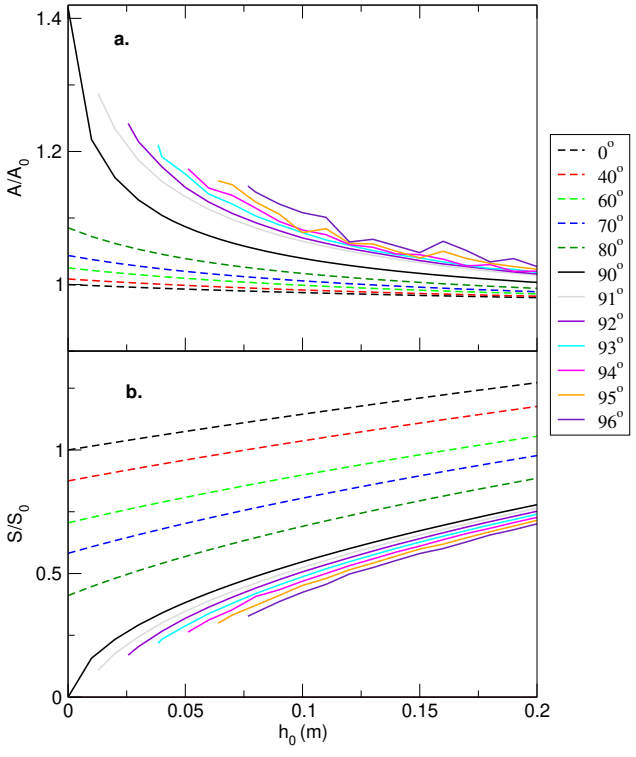


**Figure 9.** Evolution of **a.** relative constant rate $\mathrm{A}/\mathrm{A}_0$ and **b.** relative sorptivity $\mathrm{S}/\mathrm{S}_0$ versus the ponding height $h_0$ for several contact angle $\theta_w$ values, computed with PN model for $R = 50 \cdot 10^{-6}$ m and $r = 20 \cdot 10^{-6}$m.

$h_0$, the general trend of the curves was similar to those found for the cylindrical model, namely an increase of relative sorptivity $S/S_0$ and a decrease of relative constant infiltration rate $A/A_0$ towards 1, with increasing $h_0$ (figure 9).

https://doi.org/10.5194/hess-2022-193
Preprint. Discussion started: 31 May 2022


Hydrology and Earth System Sciences
Discussions

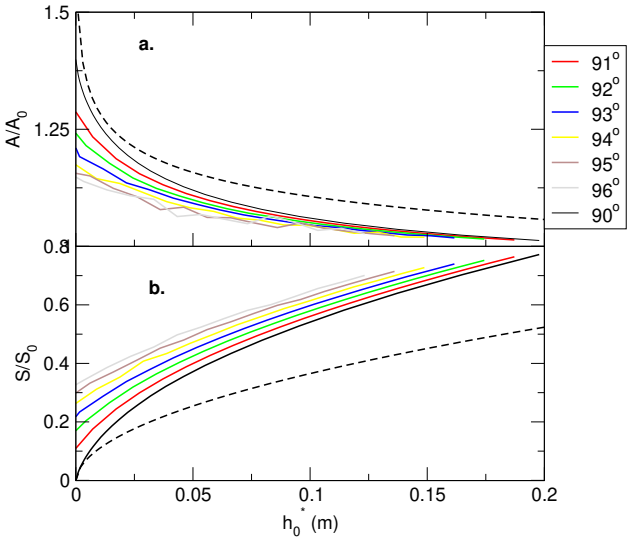


**Figure 10.** Evolution of **a.** relative constant rate and **b.** relative sorptivity rate vs relative ponding pressure $h_0^*$, computed with PN model for $R = 50 \cdot 10^{-6}$ m and $r = 20 \cdot 10^{-6}$m and several contact angle values. The dotted line represents the results for the cylindrical model with $r = 20 \cdot 10^{-6}$ m.

In comparison to the cylindrical model, the influence of contact angle $\theta_w$ was more important. Varying capillary pressure induced by varying meniscus radius during the progression along the PN model, was therefore more affected by water repellency. In fact the minimal pressure head $h_0$ necessary to initiate infiltration is governed by the pore access radius $r_a$, hence when the progressing meniscus varies between $r_a$ and $R$, capillary pressure benefits from an extra pressure head. In order to describe optimally the shape of the relation between relative infiltration parameters and relative ponding pressure, a four-parameters Hill-Langmuir equation was needed Gesztelyi et al. (2012):

$$Y = a_1 + \frac{a_2 - a_1}{1 + \left(\frac{a_3}{h_0^*}\right)^{a_4}} \tag{29}$$

The impact of ponding pressure , $h_0$, has also been evaluated for contact angles less than $90°$ and showed the same decreasing pattern with smaller variations for $A/A_0$ but a more significant linear evolution for $S/S_0$ (figure 9). Note that, on the y-axis, $h_0 = 0$, we find the impact of the contact angle on $S/S_0$ and $A/A_0$, as depicted by Figure 4 (case of moderate water repellency, $\theta_w \leq 90°$). Parameter $A$ seemed to become increasingly erratic with increasing contact angle whereas sorptivity $S$ was less affected (Figure 9 b). This can probably be explained by the fact that the computed infiltration curves started to slightly diverge from the two-terms Philip equation (Eq.1). However the general trend for $S/S_0$ and $A/A_0$ versus relative ponding pressure $h_0^*$, was equivalent to cylindrical model (Figure 10), and the optimised parameters of equation 28 were reported in table 2 and show significant differences with varying contact angle ($\theta_w$). With PN model, each contact angle value showed a specific curve for both infiltration parameters versus the ponding pressure, unlike for the cylindrical model. It means that the two effects of water pressure head and water repellency do not lump in one single effect and one related single parameter, in opposite to the case of

https://doi.org/10.5194/hess-2022-193
Preprint. Discussion started: 31 May 2022


Hydrology and Earth System Sciences
Discussions

the PN model with only $h_0^*$ playing a role. The two effects must be investigated separately for the PN model. More precisely, for a given contact angle $\theta_w$, relative ponding pressure $h_0^*$ played the same fundamental role in the infiltration kinetics as slight variations of ponding pressure, especially for small values of $h_0^*$ with a decrease and increase in $A/A_0$ and $S/S_0$ , respectively.

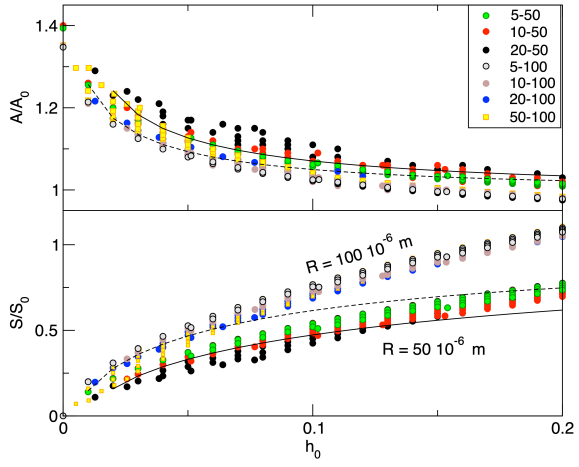


**Figure 11.** Evolution of **a.** relative constant rate and **b.** relative sorptivity rate vs ponding pressure $h_0$, computed with PN model for several combinations of $R$ and $r_a$ values for with a contact angle value of 92°. Results for cylindrical model are recalled by solid line (r = $50\times10^{-6}$m) and dotted line (r = $100 \times 10^{-6}$m).

Regarding the pore radius distribution and pore geometry, the comparison the two models PN versus cylindrical, brings more insight. Figure 11 showed clearly the chief importance of pore radius $R$ over the pore access radius $r_a$ and even over the contact angle, onto relative sorptivity($S/S_0$). Nonetheless the pore access radius $r_a$ also played a minor role on relative sorptivity $S/S_0$ as it generated scattering within each group of $R$ (Figure 11). Relative constant infiltration rate was not as much affected by the pore geometry, and mainly seemed to decrease with increasing ponding pressure. The comparison with cylindrical model highlighted consequential differences especially for the large pore radius. Moreover, within the range of commonly found pore radii in soils as shown in table 3, cylindrical model generates infiltration parameters two to three orders of magnitude higher than PN for equivalent pore sizes ($r_{cyl} = 10 \cdot 10^{-6}$, $50 \cdot 10^{-6}$ and $100 \cdot 10^{-6}$ m versus $R = 50 \cdot 10^{-6}$ and $100 \cdot 10^{-6}$ m with $r_a = 10 \cdot 10^{-6}$m). As mentioned previously (Hammecker et al., 1993; Hammecker and Jeannette, 1994; Hammecker et al., 2004), the adequacy between infiltration parameters and actual pore dimensions is far better for PN model than cylindrical pore model, though the general behaviour of both models was comparable. Nonetheless in the case of highly water repellent conditions with superficial ponding pressure, their respective behaviours diverged. Increasing pore radius for the cylindrical model led to increasing sorptivity $S$ and constant infiltration rate $A$ values, whereas increasing pore radius $R$, with constant pore access radius $r_a$ for PN model led to decreasing infiltration parameters ($A$ and $S$). As heterogeneity increased, namely the

https://doi.org/10.5194/hess-2022-193
Preprint. Discussion started: 31 May 2022


Hydrology and Earth System Sciences
Discussions

difference between pore access radius $r_a$ and actual pore radius $R$, infiltration kinetics decreased. More generally models with non uniform pore radius seemed to fit better to experimental data and to be in line with field observations as pointed out by numerous previous studies studying the variability of pore radii and exploring the adequacy of model with sinusoidal variations of pore sections (Beresnev et al., 2009; Gupta et al., 2008; Hammecker et al., 2004; Nimmo, 2013; Wang et al., 2013; Wang and Wallach, 2020, 2021).

**Table 3.** Comparison of constant infiltration rate $A$ and sorptivity $S$ for cylindrical and PN model, with a contact angle of 92°, a ponding pressure $h_0$ of 0.05m. For cylindrical model radius is $r$ and PN model $R$ and $r_a$ pore ans pore access radii.

| $r$ , $R$ (m) | $r_a$ (m) | model | $A$ $(m \cdot s^{-1})$ | $S$ $(m \cdot s^{-1/2})$ |
|---|---|---|---|---|
| $10 \cdot 10^{-}6$ | | Cyl. | $1.22 \cdot 10^{-4}$ | $2.51 \cdot 10^{-5}$ |
| $50 \cdot 10^{-6}$ | | Cyl. | $2.39 \cdot 10^{-3}$ | $1.52 \cdot 10^{-2}$ |
| $50 \cdot 10^{-6}$ | $10 \cdot 10^{-6}$ | PN | $6.31 \cdot 10^{-6}$ | $6.59 \cdot 10^{-4}$ |
| $100 \cdot 10^{-6}$ | | Cyl. | $9.49 \cdot 10^{-3}$ | $3.235 \cdot 10^{-2}$ |
| $100 \cdot 10^{-6}$ | $10 \cdot 10^{-6}$ | PN | $1.41 \cdot 10^{-6}$ | $3.97 \cdot 10^{-4}$ |

### 3.3 Consequences

These results showed that in highly water repellent conditions ($\theta_w > 90°$) ponding pressure would play an essential role to water infiltration kinetics; small variations in ponding pressure would impact highly both infiltration parameters, i.e., sorptivity and the infiltration parameter $A$. In order to keep the ponding pressure $h_0$ necessary to initiate infiltration, with reasonable height values ($h_0 < 1$ m), only contact angles values $\theta_w$ up to 96°, were considered. Considering the example of figure 8, the model showed that a difference of 0.015 m for the ponding pressure $h_0$ would lead to a difference of 0.07 m in infiltration after 10 minutes (figure 12). Soil surface roughness *i.e.* micro-relief, generating differences in ponding pressure $h_0$ during heavy rain events, can produce significant differences in progressing infiltration depth *I*, initiating development of finger flow. This type of water flow is often described in water repellent soils and more specifically in coarse textured sandy soils rather than fine textured loamy soils Wang et al. (2018), in agreement with modelling results found here.

The model highlighted that in a perfectly homogeneous porous medium, with homogeneous negative wettability values evenly distributed along the profile, heterogeneous infiltration, *i.e.,* initiation of finger flow could occur, only because of minor variations of ponding pressure. Indeed, small micro-topographic differences could induce differential infiltration rate promoting contrasting wetting front progressions. Nonetheless this process is not related to flow instability usually described to explain finger flow because of two region single phase flow or multi-phase flow or capillary pressure overshoot DiCarlo (2013). Other external parameters, like heterogeneous pore distribution in soil or varying water repellency along the soil profile Carrick et al. (2011), or time dependent contact angle due to amphiphillic molecules reorientation (Wang and Wallach, 2020, 2021) will amplify the heterogeneous and unstable infiltration resulting in fingered flow process.

https://doi.org/10.5194/hess-2022-193
Preprint. Discussion started: 31 May 2022


Hydrology and Earth System Sciences
Discussions

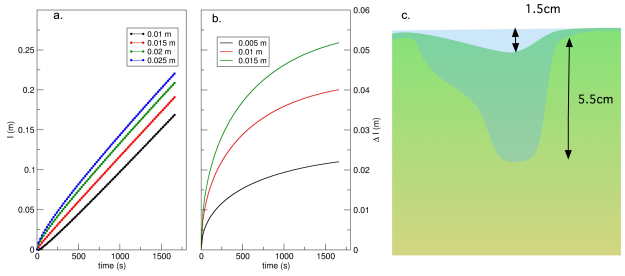


**Figure 12. a.** Raw infiltration curves for different ponding pressure $h_0$, **b.** difference in infiltration kinetics for different $h_0$ **c.** consequences on water infiltration into hydro-repellent soil for surface roughness, leading to finger shapes

## 4 Conclusions

In this study, we apply the capillary tube and pearl necklace approach for the prediction of water infiltration into water repellent soils, i.e. with contact angles different from zero. The model allowed us to generate several sets of cumulative infiltrations as a function of the contact angles below $90°$, to investigate moderate water repellency, and above $90°$, i.e. between $90°$ and $96°$, to investigate strong water repellency.

Regarding moderate water repellency, the model showed that the influence of water repellency naturally affected infiltration and as expected sorptivity $S$ declined when the contact angle $\theta_w$ increased. More surprisingly the constant infiltration rate $A$ was also affected and showed increasing values with increasing contact angle. Thought these mechanisms were not explicitly considered nor modelled here, this result is in line with physical processes and in particular the lesser friction of water along the pore walls when wettability decreases, but could also be partially due to the fact of using a truncated form of Philip equation, where $A$ increases with infiltration time. Comparing infiltration kinetics computed for cylindrical tube model with those computed for non uniform PN geometry showed comparable behaviour; especially when comparing the relative infiltration parameters $S/S_0$ and $A/A_0$. Nonetheless PN model is supposed to be more representative of real soils than cylindrical model that is based on one single pore size, and has been used to evaluate the incidence of increasing contact angle ($\theta_w$) on two major van Genuchten parameters ($\alpha$ and $K_s$). For the common values of $n$ ($2 < n < 3$) comprehensive relationships have been derived for $\alpha/\alpha_0$ versus $\cos(\theta_w)$ and $K_s/K_{s0}$ versus $\cos(\theta_w)$ where $\alpha_0$ and $K_{s0}$ refer to the parameters determined for perfectly wettable condition ($\theta_0$ = 0 °). These two van Genuchten parameters could therefore be corrected for specific contact angle values to be implemented in numerical resolution of Richard's equation for the modeling flow and water infiltration, and, more practically, could be used in general water flow models like HYDRUS.

Regarding the case of strong water repellency, i.e., when the contact angle is above $90°$, a positive water pressure head, $h_0$ is needed to initiate water infiltration at surface. As long as the water pressure head does not compensate the effect of water repellency, i.e., the term $\frac{2\sigma\cos\theta_w}{r^*\rho g}$, the water infiltration does not begin. This results is in line with field observations, when the too strong water repellency prevents any water infiltration. When the water pressure head is positive enough, the results depend on the geometry of pores. For the cylindrical model, one single relation may be obtained between cumulative infiltrations and

https://doi.org/10.5194/hess-2022-193
Preprint. Discussion started: 31 May 2022


Hydrology and Earth System Sciences
Discussions

related Philip parameters, $A$ and $S$, and the corrected water pressure head $h_0^* = h_0 + \frac{2\sigma\cos\theta_w}{r^*\rho g}$. That means that the effect of the contact angle may be perfectly compensated by a slight increase in water pressure head at surface. In opposite, for the PN model, the relation is more complex and the infiltration must be quantified as function of both the water pressure head at surface and the contact angle.

Besides, the analysis of our model brought additional insight on water infiltration into water repellent soils. It may help to explain fingered flow. Indeed, let consider any real soil, the soil surface may be characterised by a micro-relief. Consequently, at the lowest point of the surface, the water depth may be sufficient to exceed the value of the threshold needed to counterbalance water repellency. Otherwise, flow may not be initiated. The concomitance of zones with activation of infiltration nearby zones with inactivated water infiltration may explain the differential wetting front progression, source of fingering flow so often observed in water repellent soils. Our result also provided very interesting information about the incidence of different parameters, like pore geometry, contact angle and ponding pressure on infiltration kinetics in water repellent soil. Moreover it gave interesting insights to the conditions of inducing fingering flow. however experimental data would be necessary to assess and definitively validate these results.

*Author contributions.* C.H. established the question, performed the analytical developments, computed the numerical results, provided the first draft of the manuscript. L.L. checked the analytical developments, verified the numerical results and contributed to the edition of the manuscript. R.A.J. contributed to the elaboration of the project and the edition of the manuscript. S.S. contributed to the initial infiltration experiments in water repellent soils that initiated this study. All the authors contributed to the editing of the manuscript.

*Competing interests.* No competing interests to declare.

*Acknowledgements.* The authors would like to thank IRD through the program LMI LUSES, for supporting this research.

https://doi.org/10.5194/hess-2022-193
Preprint. Discussion started: 31 May 2022




## References

Abou Najm, M. R., Stewart, R. D., Di Prima, S., and Lassabatere, L.: A simple correction term to model infiltration in water-repellent soils, Water Resources Research, n/a, e2020WR028 539, https://doi.org/https://doi.org/10.1029/2020WR028539, 2021.

Angulo-Jaramillo, R., Bagarello, V., Iovino, M., and Lassabatere, L.: Infiltration Measurements for Soil Hydraulic Characterization, vol. 1, Springer International Publishing, https://doi.org/10.1007/978-3-319-31788-5, 2016.

Assouline, S.: Infiltration into soils: Conceptual approaches and solutions, Water Resour. Res., 49, 1755–1772, https://doi.org/10.1002/wrcr.20155, 2013.

Bachmann, J., Deurer, M., and Arye, G.: Modeling Water Movement in Heterogeneous Water-Repellent Soil: 1. Development of a Contact Angle Dependent Water-Retention Model, Vadose Zone J, 6, 436–445, https://doi.org/10.2136/vzj2006.0060, 2007.

Baker, R.S.and Hillel, D.: Laboratory test of a theory of figuring during infiltration into layered soils, Soil Sci. Soc. Am. J., 54, 20–30, 1990.

Bauters, T., Steenhuis, T., DiCarlo, D., Nieber, J., Dekker, L., Ritsema, C., Parlange, J.-Y., and Haverkamp, R.: Physics of water repellent soils, Journal of Hydrology, 231–232, 233–243, 2000.

Beatty, S. M. and Smith, J. E.: Fractional wettability and contact angle dynamics in burned water repellent soils, Journal of Hydrology, 391, 97–108, 2010.

Beresnev, I. A., Li, W., and Vigil, R. D.: Condition for Break-up of Non-Wetting Fluids in Sinusoidally Constricted Capillary Channels, Transport in Porous Media, 80, 581–604, 2009.

Berkowitz, B. and Balberg, I.: Percolation approach to the problem of hydraulic conductivity in porous media, Transport in Porous Media, 9, 275–286, 1992.

Berkowitz, B. and Ewing, R.: Percolation Theory and Network Modeling Applications in Soil Physics, Surveys in Geophysics, 19, 23–72, 1998.

Broadbent, S. R. and Hammersley, J. M.: Percolation processes, Mathematical Proceedings of the Cambridge Philosophical Society, 53, 629–641, https://doi.org/10.1017/s0305004100032680, 1957.

Cai, J. and Yu, B.: A Discussion of the Effect of Tortuosity on the Capillary Imbibition in Porous Media, Transport in Porous Media, 89, 251–263, https://doi.org/10.1007/s11242-011-9767-0, 2011.

Carrick, S., Buchan, G., Almond, P., and Smith, N.: Atypical early-time infiltration into a structured soil near field capacity: The dynamic interplay between sorptivity, hydrophobicity, and air encapsulation, Geoderma, 160, 579–589, 2011.

Case, C. M.: Rate of rise of liquid in capillary tube-revisited, Am. J. Phys., 58, 888–896, 1990.

Case, C. M.: Physical Principles of Flow in Unsaturated Porous Media, Oxford University Press, New York., 1994.

Chebbi, R.: Dynamics of liquid penetration into capillary tubes, Journal of Colloid and Interface Science, 315, 255–260, https://doi.org/10.1016/j.jcis.2007.06.073, 2007.

Czachor, H., Doerr, S., and Lichner, L.: Water retention of repellent and subcritical repellent soils: New insights from model and experimental investigations, Journal of Hydrology, 380, 104–111, 2010.

de Gennes, P. G.: Wetting: statics and dynamics, Rev. Mod. Phys., 57, 827–863, https://doi.org/10.1103/RevModPhys.57.827, 1985.

DeBano, L.: The role of fire and soil heating on water repellency in wildland environments: a review, Journal of Hydrology, 231—232, 195–206, 2000.

Dekker, L., Oostindie, K., and Ritsema, C.: Exponential increase of publications related to soil water repellency, Aust. J. Soil Res., 43, 403–441, 2005.

https://doi.org/10.5194/hess-2022-193
Preprint. Discussion started: 31 May 2022




Deurer, M. and Bachmann, J.: Modeling Water Movement in Heterogeneous Water-Repellent Soil: 2. A Conceptual Numerical Simulation, Vadose Zone Journal, 6, 446–457, 2007.

DiCarlo, D. A.: Stability of gravity-driven multiphase flow in porous media: 40 Years of advancements, Water Resources Research, 49, 4531–4544, https://doi.org/10.1002/wrcr.20359, 2013.

Dullien, F. A. L.: Porous Media: Fluid Transport and Pore Structure, Academic Press, New York, 1979.

Geiger, S. L. and Durnford, D. S.: Infiltration in Homogeneous Sands and a Mechanistic Model of Unstable Flow, Soil Science Society of America Journal, 64, 460–469, https://doi.org/10.2136/sssaj2000.642460x, 2000.

Gesztelyi, R., Zsuga, J., Kemeny-Beke, A., Varga, B., Juhasz, B., and Tosaki, A.: The Hill equation and the origin of quantitative pharmacology, Archive for History of Exact Sciences, 66, 427–438, https://doi.org/10.1007/s00407-012-0098-5, 2012.

Ghanbarian, B., Hunt, A. G., Sahimi, M., Ewing, R. P., and Skinner, T. E.: Percolation Theory Generates a Physically Based Description of Tortuosity in Saturated and Unsaturated Porous Media, Soil Sci. Soc. Am. J., 77, 1920–1929, https://doi.org/10.2136/sssaj2013.01.0089, 2013.

Glass, R. J., Steenhuis, T. S., and Parlange, J.-Y.: Mechanism for finger persistence in Homogeneous, unsaturated, porous media, Soil Science, 148, 60–70, https://doi.org/10.1097/00010694-198907000-00007, 1989.

Green, W. and Ampt, G.: Studies on soil physics. Part 1. The flow of air and water throuh soils., Journal of Agricultural Science, IV, 1–24, 1911.

Gupta, R. K., Abrol, I. P., Finkl, C. W., Kirkham, M. B., Arbestain, M. C., Macías, F., Chesworth, W., Germida, J. J., Loeppert, R. H., Cook, M. G., Schwab, G. O., Konstankiewicz, K., Pytka, J., Oertli, J. J., Singer, A., Edmonds, W. J., Feng, Y., Feldman, S. B., Shang, C., Zelazny, L. W., Ford, P. W., and Clothier, B. E.: Soil Pores, in: Encyclopedia of Soil Science, pp. 693–699, Springer Netherlands, https://doi.org/10.1007/978-1-4020-3995-9_548, 2008.

Hammecker, C. and Jeannette, D.: Modelling the capillary imbibition kinetics in sedimentary rocks: Role of petrographical features, Transport in Porous Media, 17, 285–303, 1994.

Hammecker, C., Mertz, J.-D., Fischer, C., and Jeannette, D.: A geometrical model for numerical simulation of capillary imbibition in sedimentary rocks, Transport in Porous Media, 12, 125–141, 1993.

Hammecker, C., Barbiéro, L., Boivin, P., Maeght, J. L., and Diaw, E. H. B.: A geometrical pore model for estimating the microscopical pore geometry of soil with infiltration measurements, Transport in Porous Media, 54, 193–219, 2004.

Hopmans, J., J.Šimůnek, Romano, N., and Durner, W.: Inverse modeling of transient water flow. Methods of soil analysis. Part 4. Physical methods., SSSA Book Ser. 5. SSSA, Madison, WI., 2002.

Huang, D. M., Sendner, C., Horinek, D., Netz, R. R., and Bocquet, L.: Water Slippage versus Contact Angle: A Quasiuniversal Relationship, Physical Review Letters, 101, 226 101, https://doi.org/10.1103/physrevlett.101.226101, 2008.

Hunt, A. G.: Comparing van Genuchten and Percolation Theoretical Formulations of the Hydraulic Properties of Unsaturated Media, Vadose Zone J, 3, 1483–1488, https://doi.org/https://doi.org/10.2136/vzj2004.1483, 2004.

Jettestuen, E., Helland, J. O., and Prodanovic, M.: A level set method for simulating capillary-controlled displacements at the pore scale with nonzero contact angles, Water Resour. Res., 49, 4645–4661, 2013.

Kutilek, M. and Nielsen, D. R.: Soil Hydrology, Catena Verlag, 1994.

Lassabatere, L., Angulo-Jaramillo, R., Goutaland, D., Letellier, L., Gaudet, J., Winiarski, T., and Delolme, C.: Effect of the settlement of sediments on water infiltration in two urban infiltration basins, Geoderma, 156, 316–325, https://doi.org/10.1016/j.geoderma.2010.02.031, 2010.


Lassabatere, L., Loizeau, S., Angulo-Jaramillo, R., Winiarski, T., Rossier, Y., Delolme, C., and Gaudet, J. P.: Influence of the initial soil water content on Beerkan water infiltration experiments, in: EGU General Assembly Conference Abstracts, EGU General Assembly Conference Abstracts, p. 2278, 2012.

Le Besnerais, P.: Impact de l'hévéaculture sur les propriétés hydrodynamiques du sol., Master's thesis, Institut National d'Horticulture et de Paysage, Angers., 2011.

Mao, J., Nierop, K. G. J., Rietkerk, M., and Dekker, S. C.: Predicting soil water repellency using hydrophobic organic compounds and their vegetation origin, SOIL, 1, 411–425, https://doi.org/10.5194/soil-1-411-2015, 2015.

Ma'Shum, M., Tate, M. E., Jones, G. P., and Oades, J. M.: Extraction and characterization of water-repellent materials from Australian soils, Journal of Soil Science, 39, 99–110, https://doi.org/10.1111/j.1365-2389.1988.tb01198.x, 1988.

Mualem, Y.: A new model for predicting the hydraulic conductivity of unsaturated porous media., Water Resources Research, 12, 513–522, 1976.

Mukunoki, T., Miyata, Y., Mikami, K., and Shiota, E.: X-ray CT analysis of pore structure in sand, Solid Earth, 7, 929–942, https://doi.org/10.5194/se-7-929-2016, 2016.

Neto, C., Evans, D. R., Bonaccurso, E., Butt, H.-J., and Craig, V. S. J.: Boundary slip in Newtonian liquids: a review of experimental studies, Reports on Progress in Physics, 68, 2859–2897, https://doi.org/10.1088/0034-4885/68/12/r05, 2005.

Nimmo, J.: Porosity and Pore Size Distribution, in: Reference Module in Earth Systems and Environmental Sciences, Elsevier, https://doi.org/10.1016/b978-0-12-409548-9.05265-9, 2013.

Nissan, A., Wang, Q., and Wallach, R.: Kinetics of gravity-driven slug flow in partially wettable capillaries of varying cross section, Water Resources Research, 52, 8472–8486, https://doi.org/10.1002/2016wr018849, 2016.

Nyman, P., Sheridan, G., and Lane, P. N. J.: Synergistic effects of water repellency and macropore flow on the hydraulic conductivity of a burned forest soil, south-east Australia, Hydrological Processes, 24, 2871–2887, https://doi.org/10.1002/hyp.7701, 2010.

Parlange, J.-Y.: On Solving the Flow Equation in Unsaturated Soils by Optimization: Horizontal Infiltration, Soil Science Society Of America Journal, 39, 415–418, 1975.

Peiris, M. G. C. and Tennakone, K.: Rate of rise of a liquid in a capillary tube, American Journal of Physics, 48, 415–415, https://doi.org/10.1119/1.12099, 1980.

Philip, J.: The theory of infiltration: 4. sorptivity and algebraic infiltration equations., Soil Science, 84, 257–264, 1957.

Prodanović, M. and Bryant, S. L.: A level set method for determining critical curvatures for drainage and imbibition, Journal of Colloid and Interface Science, 304, 442–458, https://doi.org/10.1016/j.jcis.2006.08.048, 2006.

Richards, L.: Capillary conduction of liquids through porous mediums, Journal of Applied Physics, 1, 318–333, https://doi.org/10.1063/1.1745010, 1931.

Ritsema, C. J., Dekker, L. W., Hendrickx, J. M. H., and Hamminga, W.: Preferential flow mechanism in a water repellent sandy soil, Water Resources Research, 29, 2183–2193, https://doi.org/10.1029/93wr00394, 1993.

Šimůnek, J., Wendroth, O., and van Genuchten, M.: Parameter estimation analysis of the evaporation method for determining soil hydraulic properties, Soil Sci Soc Am J, 62, 894–905, 1998.

Šimůnek, J., Šejna, M., Saito, H., Sakai, M., and van Genuchten, M. T.: The hydrus-1d software package for simulating the movement of water, heat, and multiple solutes in variably saturated media, version 4.16, Hydrus software series 3, Department of Environmental Sciences, University of California Riverside, University of California Riverside , California, USA, 2013.

Sutera, S. and Skalak, R.: The history of Poiseuille's law, Annual Review of Fluid Mechanics, 25, 1–19, 1993.

https://doi.org/10.5194/hess-2022-193
Preprint. Discussion started: 31 May 2022




van Genuchten, M.: A closed-form equation for predicting the hydraulic conductivity of unsaturated soils, Soil Science Society of America Journal, 44, 892–898, 1980.

Wallach, R. and Jortzick, C.: Unstable finger-like flow in water-repellent soils during wetting and redistribution – The case of a point water source, Journal of Hydrology, 351, 26 – 41, https://doi.org/10.1016/j.jhydrol.2007.11.032, 2008.

Wang, Q., Graber, E. R., and Wallach, R.: Synergistic effects of geometry, inertia, and dynamic contact angle on wetting and dewetting of capillaries of varying cross sections, Journal of Colloid and Interface Science, 396, 270–277, 2013.

Wang, Y., Wang, X., Chau, H. W., Si, B., Yao, N., and Li, Y.: Water Movement and Finger Flow Characterization in Homogeneous Water-Repellent Soils, Vadose Zone Journal, 17, 1–12, https://doi.org/10.2136/vzj2018.01.0021, 2018.

Wang, Z. and Wallach, R.: Effects of Time-Dependent Contact Angle on Wettability of Subcritically Water-Repellent Soils, Water Resources Research, 56, https://doi.org/10.1029/2020wr027314, 2020.

Wang, Z. and Wallach, R.: Water infiltration into subcritical water-repellent soils with time-dependent contact angle, Journal of Hydrology, 595, 126 044, https://doi.org/10.1016/j.jhydrol.2021.126044, 2021.

Wang, Z., Wu, Q., Wu, L., Ritsema, C., Dekker, L., and Feyen, J.: Effects of soil water repellency on infiltration rate and flow instability, Journal of Hydrology, 231-232, 265–276, 2000.

Washburn, E. W.: The Dynamics of Capillary Flow, Phys. Rev., 17, 273–283, 1921.